

# Orientation of rigid rods dissolved in deformed networks

B. Erman,\* J. P. Jarry† and L. Monnerie

Laboratoire de Physicochimie Structurale et Macromoléculaire, associé au CNRS, ESPCI,  
10 rue Vauquelin, 75231 Paris Cedex 05, France

(Received 16 October 1986; accepted 6 November 1986)

Orientations of three rigid diphenylpolyene probes of different lengths (1.15, 1.4 and 1.65 nm) in uniaxially deformed *cis*-1,4-polyisoprene networks are determined by fluorescence polarization measurements. The degree of coupling between the probes and the network is explained by a theoretical model, leading to the expression  $f = f_0 + f_2 S^2$ , where  $f_0$  and  $f$  show the degree of coupling in the undeformed and deformed networks, respectively,  $f_2$  is a coefficient to be determined experimentally and  $S$  is the orientation function for the network. The degree of coupling of the probes to the network chains varied inversely with probe lengths but was independent of temperature changes and the degree of swelling. A likely molecular origin of the coupling of polyisoprene chains with the probes would involve the statistically favourable *skew*<sup>±</sup>, *trans,skew*<sup>±</sup> sequences.

(Keywords: orientation; polyisoprene; network; fluorescence polarization)

## INTRODUCTION

Chain segments in an amorphous polymeric network orient under a macroscopically applied deformation. The degree of orientation of the segments may conveniently be described by the second Legendre polynomial, or the equilibrium orientation function  $S$ , defined as:

$$S = \frac{1}{2}(3\langle \cos^2 \theta \rangle - 1) \quad (1)$$

where  $\theta$  denotes the angle between a laboratory-fixed axis and the direction of a segment, or of a specific vector affixed to the segment. The angular brackets denote the average over all segments of interest. Recently, the relationship of the orientation function to the state of macroscopic deformation and to the molecular constitution of networks has been presented in the form of a general theory<sup>1</sup>. The predictions were seen to be in satisfactory agreement with results of orientation measurements on deformed *cis*-polyisoprene networks<sup>2</sup>. The measurements were performed on networks in which a small amount of chains were labelled with dimethylene anthracene (DMA) fluorescent groups. Determination of the orientations of the DMA groups by the fluorescence polarization technique leads to the evaluation of  $S$  at different levels of strain, swelling and temperature.

In the present paper, we report and discuss the degree of orientation of rigid rods dissolved in deformed networks<sup>3</sup>. In contrast to the DMA groups, which are labels affixed to the network chains, the rigid rods are probes which are chemically 'unattached' to the network structure. The orientations of these probes upon deformation of the network are realized through local intermolecular correlations with the orienting sequences

of the polyisoprene network chains. The major interest of the present study is to determine the degree of coupling of the probes to their environments, and the effect of strain, swelling temperature and probe length on this coupling.

## EXPERIMENTAL

### Materials

The commercially available polymer investigated is an anionic polyisoprene (Shell IR 307) of high molecular weight ( $M_n \approx 500\,000$ ) with high *cis*-1,4 configuration (92%). It was carefully purified by extraction with ethanol as a solvent and mixed with small amounts of dicumyl peroxide as a crosslinking agent. Samples were moulded and crosslinked at 147°C. Probes and label were added as follows:

(a) Three probes of varying size were employed: diphenylbutadiene (DPBD), diphenylhexatriene (DPHT) and diphenyloctatetraene (DPOT). Their formula and transition moments are shown in Figure 1. Crosslinked IR 307 samples were swollen with solutions of the probes in benzene and then dried *in vacuo*. The final probe concentration in bulk samples was approximately  $2 \times 10^{-5}$  M.

(b) The synthesis of anthracene-labelled (DMA) polyisoprene chains (shown in Figure 1) is performed by preparing monofunctional anionically 'living' chains and deactivating them by 9,10-bis(bromomethyl)anthracene. The labelled polymer (1 g) and purified IR 307 polyisoprene (99 g) were mixed in solution before adding dicumyl peroxide. The final concentration of DMA in bulk samples was  $10^{-5}$  M.

Some experiments have been performed on samples swollen by toluene.

### Measurement technique

Orientation measurements of labelled chains and probes have been performed by fluorescence polarization.

\* Permanent address: School of Engineering, Bogazici University, Bebek, Istanbul, Turkey.

† Permanent address: Rhône-Poulenc Films, Usine de St-Maurice de Beynost, 01700 Miribel, France.

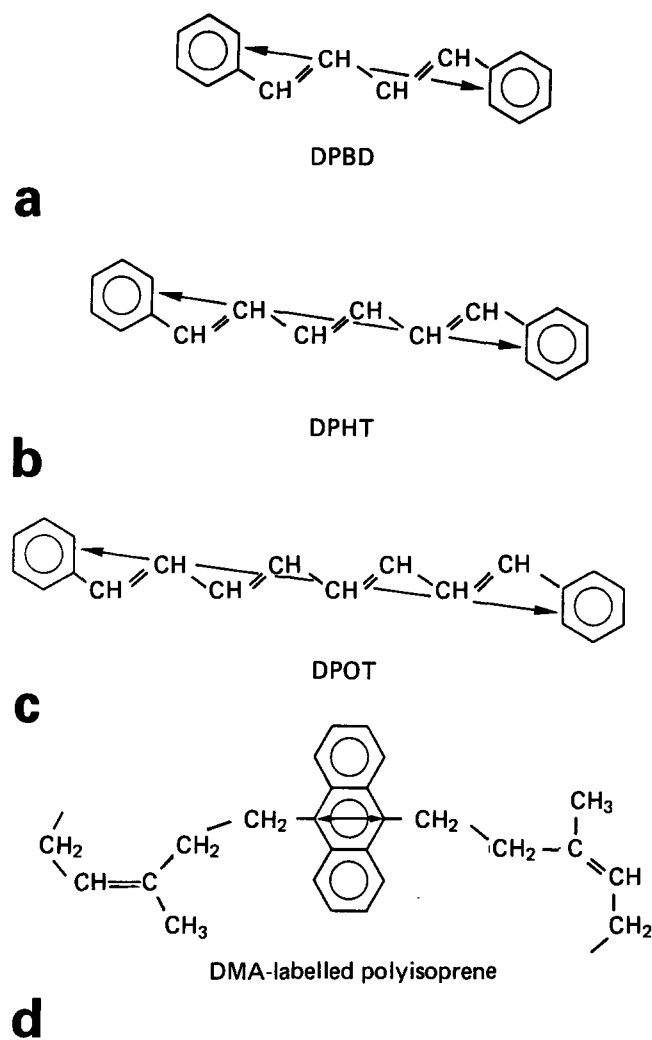


**Figure 1** Molecular structure of the three rigid probes: (a) diphenylbutadiene (DPBD), (b) diphenylhexatriene (DPHT) and (c) diphenyloctatetraene (DPOT); and (d) molecular structure of anthracene-labelled (DMA) polyisoprene

The theory of this technique has been extended to the case of a uniaxial distribution of moving molecules<sup>4</sup>. It provides a measure of the orientation function  $S$ , defined by equation (1), where  $\theta$  denotes the angle between the stretching direction and the transition moment of the label or the probe molecules.

The fluorescence polarization apparatus used has been described elsewhere<sup>5</sup>. It permits simultaneous measurements of stress and orientation during stretching. Values of the orientation function  $S$  were obtained after correcting for the effect of delocalization of the transition moments according to the theory presented in ref. 4. For this purpose, additional measurements of the limiting anisotropy  $r_0$  were carried out by fluorescence anisotropy decay experiments on undeformed samples.

The deformation ratio  $\alpha$  denotes the ratio of the final length of the sample to the initial swollen length.

## RESULTS OF MEASUREMENTS

Results of orientation measurements of the deformed network and of the probes are presented in Figures 2-4. The points represent experimental data. The curves are obtained from the theory explained in the following section.

In Figure 2, values of the orientation function are plotted in terms of the elongation ratio  $\alpha$ . The upper set of points denote the values of  $S$  obtained from networks with DMA only. These points are representative of the orientation of segments of the network chains. The sets of points labelled as A, B and C show, respectively, the orientation functions of DPBD, DPHT and DPOT in the deformed networks.

The effect of swelling on orientation is shown in Figure 3 where values of  $S$  are shown for DPOT in the unswollen and swollen networks.

In Figure 4, the ratio  $f$  of the orientation function of the probes to that of the labels in the network is shown as a function of  $\alpha$ , for the three types of probes. The data sets labelled as A, B and C refer to DPBD, DPHT and DPOT, respectively.

## ANALYSIS OF RESULTS

### The orientation function for the network

The following is a brief review of the orientation function for a real network. For details, the reader is referred to ref. 1.

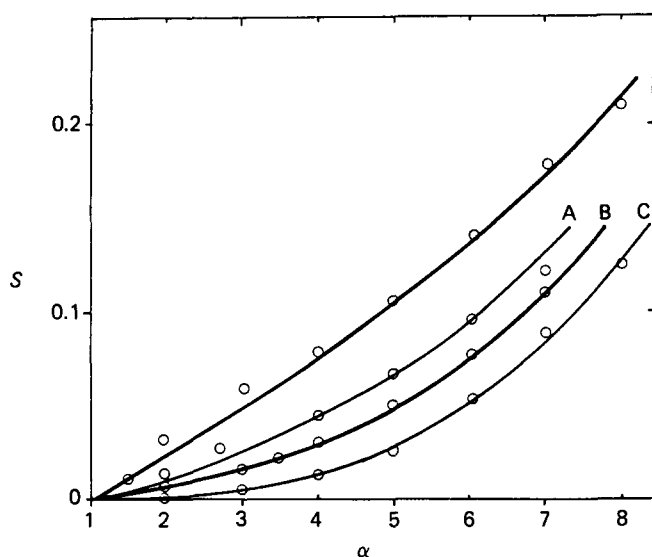


**Figure 2** Values of the orientation function plotted against the elongation ratio  $\alpha$ . Points represent experimental data. Curves are obtained from theory. The upper set of data are obtained from networks labelled with DMA. The three sets labelled A, B and C are obtained from networks containing DPBD, DPHT and DPOT, respectively

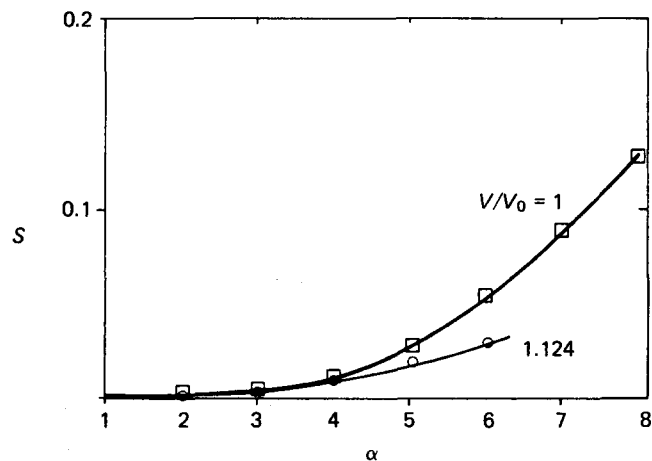


**Figure 3** Effect of swelling on orientation of DPOT in the network. Orientation function for probes is shown as a function of extension ratio  $\alpha$ , for the unswollen ( $V/V_0=1$ ) and swollen ( $V/V_0=1.124$ ) networks. Points represent experimental data. Curves are obtained by theory

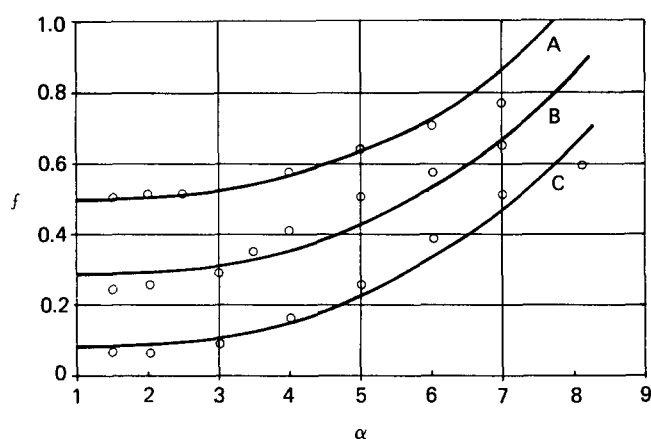


**Figure 4** The ratio of the orientation function of the probes to that of the labels in the network versus extension ratio. Points represented by the sets A, B and C are experimental data for DPBD, DPHT and DPOT, respectively. Curves are obtained by theory

The state of macroscopic deformation for a network may be described by the displacement gradient tensor  $\lambda$ . For simple extension along a laboratory-fixed  $x$ -axis,  $\lambda$  is expressed as the diagonal matrix

$$\lambda = \begin{bmatrix} \lambda_x & & \\ & \lambda_y & \\ & & \lambda_z \end{bmatrix} = \begin{bmatrix} \lambda & & \\ & (V/V_0\lambda)^{1/2} & \\ & & (V/V_0\lambda)^{1/2} \end{bmatrix} \quad (2)$$

Here,  $\lambda_x \equiv \lambda$  denotes the ratio of the final length of the sample to the initial undeformed length at unswollen volume  $V_0$ ,  $V$  is the final volume and  $\lambda_y = \lambda_z$  are the lateral deformation ratios. The deformation ratio  $\alpha$  denotes the ratio of the final length of the sample to the initial swollen length. Thus,  $\alpha$  is related to  $\lambda$  as:

$$\alpha = (V/V_0)\lambda \quad (3)$$

The state of deformation at the molecular level in the network is defined<sup>1,6</sup> by two microscopic deformation tensors,  $\Lambda^2$  and  $\Theta^2$ :

$$\Lambda^2 = \begin{bmatrix} \Lambda_x^2 & & \\ & \Lambda_y^2 & \\ & & \Lambda_z^2 \end{bmatrix} \quad \mathcal{H}^2 = \begin{bmatrix} \Theta_x^2 & & \\ & \Theta_y^2 & \\ & & \Theta_z^2 \end{bmatrix} \quad (4)$$

where

$$\Lambda_t^2 = (1 - 2/\phi)\lambda_t^2 + (2/\phi)(1 + B_t) \quad (5)$$

$$\Theta_t^2 = 1 + g_t B_t \quad (6)$$

Here,

$$B_t = (\lambda_t - 1)(\lambda_t + 1 - \zeta\lambda_t^2)/(1 + g_t)^2 \quad (7)$$

with

$$g_t = \lambda_t^2 [\kappa^{-1} + \zeta(\lambda_t - 1)] \quad (8)$$

where  $t$  indicates  $x$ ,  $y$  or  $z$ , and the two coefficients  $\kappa$  and  $\zeta$  are the elastic parameters of the network as described previously<sup>6</sup>. The tensor  $\Lambda^2$  reflects the non-affine transformations of the network chains. The transformations of the constraint domains are represented by

$\Theta^2$ . Both  $\Lambda^2$  and  $\Theta^2$  are representative of the elastic mechanisms operating in a deformed real network.

For a network under simple extension, the orientation function is given as<sup>1</sup>:

$$S = D[\Lambda_x^2 - \Lambda_y^2 + e(\Theta_x^2 - \Theta_y^2)] \quad (9)$$

Here,  $D$  represents the coefficient of orientation, which is a function of the constitution of the individual chains of the network and of intermolecular correlations<sup>1</sup>, and  $e$  is an empirical coefficient reflecting the effect of local constraints on segmental orientation.

The curve through the upper set of data points in Figure 2, representing segmental orientation in the network used in this study, is obtained by using equation (9). The network chains had an average molecular weight of  $1.9 \times 10^4$  between crosslinks, and the values of  $\kappa$ ,  $\zeta$ ,  $D$  and  $e$  were previously obtained<sup>8</sup> from stress-strain and orientation experiments as:

$$\begin{aligned} \kappa &= 9 \\ \zeta &= 0.025 \\ D &= \begin{cases} 0.006 & \text{for } V_0/V = 1 \\ 0.0035 & \text{for } V_0/V = 0.89 \end{cases} \quad (10) \\ e &= 1.4 \end{aligned}$$

#### Formulation of the function $f$

The function  $f$  represents the ratio of the orientation function for the probes to that of the labels. Previous work<sup>1</sup> has indicated that the orientation function for the labels is representative of the orientation function for the network matrix. Hence,  $f$  may be regarded as representing the degree of coupling of the probes to the network matrix. A value of  $f=0$  indicates no coupling, whereas  $f=1$  shows that the probes are perfectly correlated with the chains of the network. In the latter case they may be perfectly correlated with the chains of the network. Experimental data presented in Figure 4 show that coupling of the probes to the surrounding chains increases with deformation. Extrapolation of the data points to  $\alpha=1$  shows the degree of coupling in the state of rest. The data also show that the degree of coupling decreases with the length of the probe.

The correlation or coupling of the rods with their oriented environments may be represented as:

$$f = f_0 + F(\alpha) \quad (11)$$

where  $f_0$  is the degree of coupling in the state of rest and  $F(\alpha)$  is the contribution from deformation.  $F(\alpha)$  may be developed into a Taylor series in terms of powers of  $S$ , leading to:

$$f = f_0 + f_1 S + f_2 S^2 + f_3 S^3 + \dots \quad (12)$$

Inasmuch as the minimum degree of coupling should occur in the undistorted state,  $f_1$  must be zero. Equation (12) may then be written, to the first-order approximation, as:

$$f = f_0 + f_2 S^2 \quad (13)$$

The two coefficients in equation (13) have to be evaluated from experiment. The value of  $f_2$  should be independent of probe characteristics inasmuch as it is a coefficient reflecting the effect of orientation in the

surrounding network. The orientation function  $S$  appearing in equation (13) is given by equation (9), which refers to the average orientation field surrounding the probes. Calculations based on this function are presented in the next section. If, however, an affine network is assumed, equation (13) simplifies to:

$$f = f_0 + f_2(V/V_0)^{4/3}D^2(\alpha^4 - 2\alpha + \alpha^{-2}) \quad (14)$$

Although equation (14) is a simpler expression than would result by the use of equation (9) for  $S$ , it does not reflect all features of local orientation in real networks as was discussed previously<sup>1,2</sup>.

#### Evaluation of $f_0$ and $f_2$ from experimental data and numerical calculations

Using the data set given in equation (10), values of  $S$  can be evaluated for the network by using equation (9). The curve passing through the upper set of data points in Figure 2 is obtained in this manner. Numerical values for  $f_0$  and  $f_2$  of equation (13) may then be chosen by trial to give the best agreement to data points in Figure 4. Calculations performed on this basis lead to  $f_2 = 12$ , and  $f_0 = 0.5, 0.3$  and  $0.1$  for DPBD, DPHT and DPOT, respectively. Results of calculations using these values of  $f_0$  and  $f_2$  in equation (13) are shown by the three curves in Figure 4. Determination of the function  $f$  then leads to the calculation of the absolute orientations of probes. Results of calculations of the orientation functions for the probes are shown by the lower three curves in Figure 2. The orientation function for the probes in the swollen network may similarly be calculated. The lower curve in Figure 3 is calculated from equation (9) by using the data of equation (10) corresponding to the swollen network.

## DISCUSSION

Experimental values of the coupling function  $f$ , shown in Figure 4, change insignificantly at deformations below  $\alpha = 3$ , and increase relatively rapidly for deformations above  $\alpha = 3$ . The theoretical prediction of  $f$  based on the assumption that  $f$  varies with the square of the network orientation function is in good agreement with data.

The dependence of  $f_0$  on probe length is shown in Figure 5, in which the degree of coupling  $f_0$  in the undeformed network is plotted as a function of probe length for the three probes. The three points lie on a straight line which extrapolates to a length of 0.55 nm for full correlation,  $f_0 = 1$ .

It should be noted that neither temperature nor swelling significantly affect the degree of coupling between the probes and the network, as shown in Figure 6. Changing the temperature between  $-30^\circ\text{C}$  and  $85^\circ\text{C}$  was observed to have no marked effect on the orientation functions and therefore on the ratio  $f$ . At  $-47^\circ\text{C}$ , a marked increase was observed in the value of  $S$ , but the ratio  $f$  was not significantly affected. In Figure 6, the curves are representative of all data obtained in the range of temperatures,  $-30^\circ\text{C} < T < 85^\circ\text{C}$ , for DPBT and DPHT. The broken curves correspond to experimental results at  $-47^\circ\text{C}$ , indicating that the degree of coupling of the probes to the network does not depend significantly on temperature. Data for DPOT also showed a similar trend and are not shown in the figure for the sake of clarity. Curves for the degree of coupling in swollen

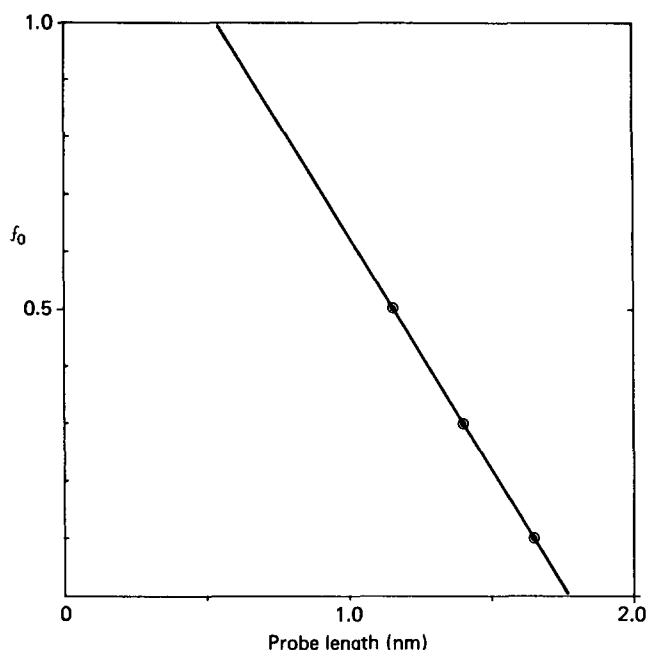


Figure 5 Dependence of the strain-independent part of the coupling function on probe length

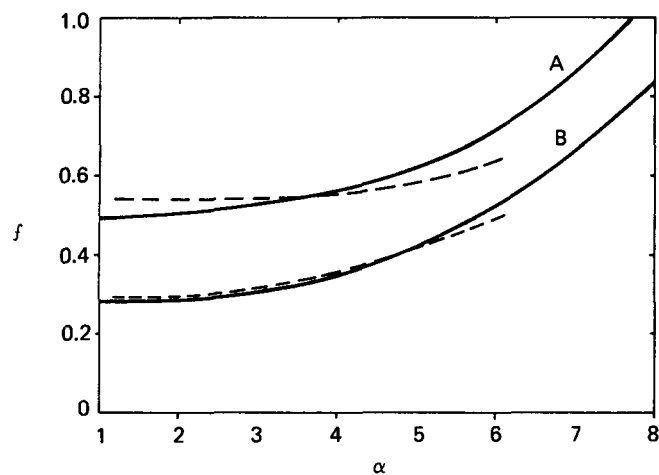
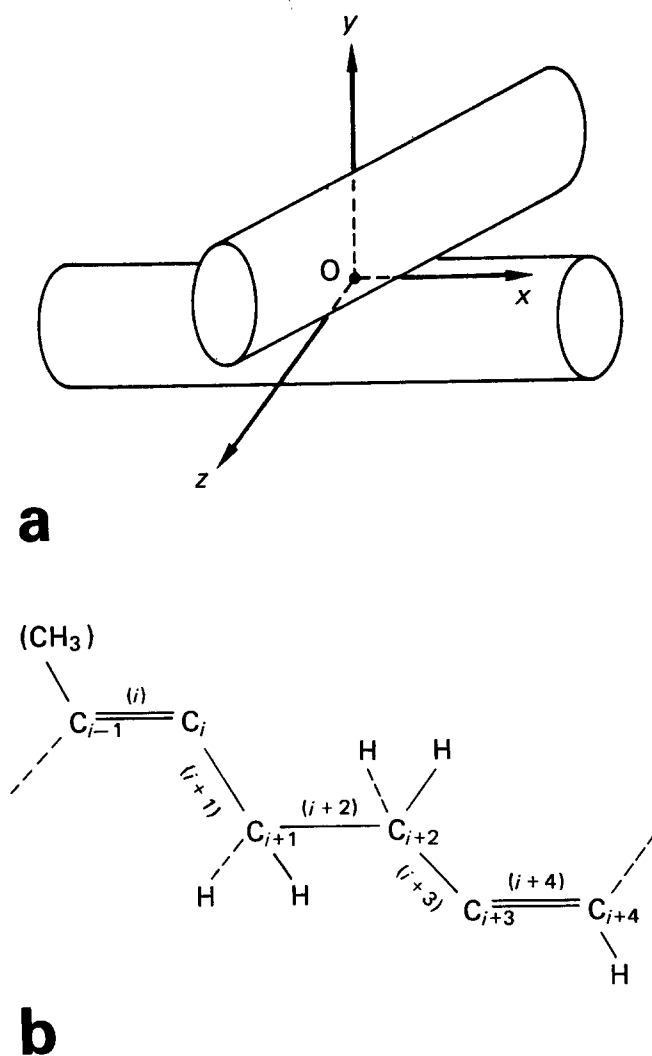


Figure 6 Effect of temperature on the coupling function for DPBT (curves A) and DPHT (curves B). Full curves indicate results at  $T = 25^\circ\text{C}$  and broken curves those at  $T = -47^\circ\text{C}$

networks ( $V/V_0 = 1.124$ ) coincided with those for unswollen networks.

At this point it is worthwhile to address the question of the molecular origin of the orientation coupling of the free rigid probe with its oriented surrounding. The presence of local orientational correlations in polymeric liquids in the state of rest has been established by previous experiments. Depolarized Rayleigh scattering by liquid n-alkanes<sup>9-12</sup> as well as birefringence experiments on various crosslinked networks<sup>7,13-17</sup> and fluorescence polarization measurements<sup>2</sup> clearly show the effects of orientational correlations among anisotropic sequences. It has furthermore been shown that a rigid fluorescent probe dispersed in a poly(ethylene terephthalate) film which is subsequently stretched above its glass transition temperature orients similar to the *trans* sequences of the polymer chain<sup>18</sup>.

The degree of correlations among the *trans* sequences of neighbouring n-alkane chains in the melt has quantitatively been analysed by Flory<sup>19</sup> a few years ago. According to the analysis, the prerequisite for enhanced



**Figure 7** (a) Two neighbouring sequences approximated by cylindrical rods. Point O is the point of contact. The x-axis is along one of the cylinders. The xz plane is the mutual plane of contact. The y-axis represents the axis about which rotation of one rod may take place relative to the other. (b) A repeat unit of the *cis*-1,4-polyisoprene chain where bonds  $(i+1)$ ,  $(i+2)$  and  $(i+3)$  are in *trans* conformations

correlations is the presence of long *trans* sequences in the melt. It is shown that orientational correlations among two correlated sequences is significant. Two *trans* sequences are depicted in Figure 7a in the form of two rods in contact. The x-axis is chosen along one and the y-axis is normal to the mutual tangent plane xz at the point of contact. The contributions to these short-range orientational correlations arise mainly from two sources. First, steric inhibitions among two such neighbouring sequences limit their relative orientations. Relative orientation changes can occur, without steric constraints, only about the y-axis. Secondly, all the orientations about this axis are not equally probable, resulting in further orientational correlations among the longitudinal directions of the *trans* sequences.

The long sequence of *trans* bonds of the three diphenylpolyene probes used in the present study conform to the requirement of anisotropy for correlations with neighbouring molecules. These rods are surrounded by sequences of *cis*-1,4-polyisoprene chains of the network. A repeat unit of the *cis*-polyisoprene chain commencing with the  $i$ th bond is schematically shown in

Figure 7b. The  $(i+1)$ th bond can take conformations *skew*<sup>±</sup> ( $s^\pm$ ) and *trans* ( $t$ ) according to theory<sup>20</sup>. The bond  $(i+2)$  can take the usual *trans* and *gauche*<sup>±</sup> conformations, and the bond  $(i+3)$  can take the *skew*<sup>±</sup> conformations. According to theory<sup>20</sup> the *skew* conformations for the bond  $(i+1)$  as well as bond  $(i+3)$  may be taken to be  $\pm 60^\circ$ . In the most probable conformation where the two double bonds  $(i)$  and  $(i+4)$  are parallel, and bonds  $(i+1)$ ,  $(i+2)$  and  $(i+3)$  are at  $s^\pm$ ,  $t$  and  $s^\mp$ , respectively, the distance between  $C_{i-1}$  and  $C_{i+3}$  is 0.573 nm, which is very close to the length of 0.603 nm of the all-*trans* state, and the chain contour from  $C_{i-1}$  to  $C_{i+4}$  is rectilinear. The  $s^\pm t s^\mp$  sequence of the *cis*-1,4-polyisoprene repeat units thus qualifies as the anisotropic sequences surrounding the rigid rods.

The correlations or coupling of the rods with their environments may be taken to be proportional to the probability of  $s^\pm t s^\mp$  sequences surrounding the rods. The degree of correlation has therefore to decrease with increasing length of the rods, as experimentally observed and shown in Figure 5.

The assignment of  $s^\pm t s^\mp$  sequences as the major source of correlations with the diphenylpolydiene is further supported by the value of 0.55 nm obtained from extrapolation of the straight line in Figure 5 to  $f_0 = 1$ .

If orientational correlations between the diene probes and the  $s^\pm t s^\mp$  sequences are accepted as the major source, then the increase of  $f$  with deformation may be construed to reflect the preferential orientation of the  $s^\pm t s^\mp$  sequences under strain. In fact, calculations of Abe and Flory<sup>20</sup> show that the double bonds in the *cis*-1,4-polyisoprene chains exhibit strong preferential orientation along the direction of stretch. Inasmuch as the  $s^\pm t s^\mp$  sequences contain two parallel double bonds, they are expected to align preferentially along the direction of stretch. The increase in the population of these sequences along the stretch direction will therefore enhance the alignment of the probes.

The preceding discussion is in agreement with experimental data shown in Figure 4. The empirical parameter  $f_2$  in equation (13) reflects the effects of preferential orientation of the appropriate chain sequence on the behaviour of the probes.

## ACKNOWLEDGEMENT

This work was supported by NATO Grant No. 85-0367.

## REFERENCES

- 1 Erman, B. and Monnerie, L. *Macromolecules* 1985, **18**, 1985
- 2 Queslel, J. P., Erman, B. and Monnerie, L. *Macromolecules* 1985, **18**, 1991
- 3 Jarry, J. P. Thèse Doctorat ès-Sciences, Université Pierre et Marie Curie, Paris, 1978
- 4 Jarry, J. P. and Monnerie, L. *J. Polym. Sci., Polym. Phys. Edn.* 1978, **16**, 443
- 5 Jarry, J. P., Pambrun, C., Sergot, Ph. and Monnerie, L. *J. Phys. E.* 1978, **11**, 702
- 6 Erman, B. and Flory, P. J. *Macromolecules* 1983, **16**, 1601
- 7 Erman, B. and Flory, P. J. *Macromolecules* 1983, **16**, 1607
- 8 Jarry, J. P., Erman, B. and Monnerie, L. *Macromolecules* 1986, **19**, 2755
- 9 Quinones, H. and Bothorel, P. C. *R. Acad. Sci. Paris* 1973, **277**, 133
- 10 Lemaire, B., Fourche, G. and Bothorel, P. C. *R. Acad. Sci. Paris* 1972, **274**, 1481
- 11 Fisher, E. W., Strobl, G. R., Dettenmaier, M., Stamm, M. and Steidle, N. *Faraday Disc. Chem. Soc.* 1979, **68**, 26

- |    |  |    |   |
|----|--|----|---|
| 12 | Patterson, G. D. and Flory, P. J. <i>J. Chem. Soc., Faraday Trans. II</i> 1972, <b>68</b> , 1098 | 16 | Gent, A. N. <i>Macromolecules</i> 1969, <b>2</b> , 262  |
| 13 | Fukuda, M., Wilkes, G. L. and Stein, R. S. <i>J. Polym. Sci. (A-2)</i> 1971, <b>9</b> , 1417     | 17 | Liberman, M. H., Abe, Y. and Flory, P. J. <i>Macromolecules</i> 1972, <b>5</b> , 550                      |
| 14 | Ishikawa, T. and Nagai, K. <i>J. Polym. Sci. (A-2)</i> 1969, <b>7</b> , 1123                     | 18 | Nobbs, J. H., Bower, D. I. and Ward, I. M. <i>J. Polym. Sci., Polym. Phys. Edn.</i> 1979, <b>17</b> , 259 |
| 15 | Rehage, G., Schäfer, E. E. and Schwarz, J. <i>Angew. Makromol. Chem.</i> 1971, <b>16</b> , 231   | 19 | Flory, P. J. <i>Faraday Disc. Chem. Soc.</i> 1979, <b>68</b> , 14   |
|    |  | 20 | Abe, Y. and Flory, P. J. <i>J. Chem. Phys.</i> 1971, <b>4</b> , 230                                       |